

Concurrence of directional Kondo transport and incommensurate magnetic order in the layered material AgCrSe₂

José Guimarães,^{1,2} Dorsa S. Fartab,¹ Michal Moravec,^{1,2} Marcus Schmidt,¹ Michael Baenitz,¹ Burkhard Schmidt,¹ and Haijing Zhang^{1,*}

¹*Max Planck Institute for Chemical Physics of Solids, 01187 Dresden, Germany*

²*School of Physics and Astronomy, University of St Andrews, St Andrews KY16 9SS, UK*

ABSTRACT

In this work, we report on the concurrent emergence of the directional Kondo behavior and incommensurate magnetic ordering in a layered material. We employ temperature- and magnetic field-dependent resistivity measurements, susceptibility measurements, and high resolution wavelength X-ray diffraction spectroscopy to study the electronic properties of AgCrSe₂. Impurity Kondo behavior with a characteristic temperature of $T_K = 32$ K is identified through quantitative analysis of the in-plane resistivity, substantiated by magneto-transport measurements. The agreement between our experimental data and the Schlottmann's scaling theory allows us to determine the impurity spin as $S = 3/2$. Furthermore, we discuss the origin of the Kondo behavior and its relation to the material's antiferromagnetic transition. Our study uncovers an unusual phenomenon—the equivalence of the Néel temperature and the Kondo temperature—paving the way for further investigations into the intricate interplay between impurity physics and magnetic phenomena in quantum materials, with potential applications in advanced electronic and magnetic devices.

INTRODUCTION

Layered quantum materials, consisting of alternating sheets of magnetic rare earth or transition metal ions on a triangular lattice and nonmagnetic transition metal planes, comprise a unique combination of magnetic frustration and highly anisotropic transport properties. These materials exhibit a plethora of unconventional properties, such as various types of magnetic order [1, 2], giant magnetoresistance [3, 4] and skyrmions [5], which arise from the combined effects of the magnetic order and electron correlations. Investigating how the electronic degrees of freedom couple with the magnetic order in such systems is key to understanding the microscopic mechanisms of the observed physical phenomena.

AgCrSe₂ is a member of the class of intercalated transition metal dichalcogenides where CrSe₂ transition metal dichalcogenide layers alternate with transition metal Ag layers. It has been recently demonstrated to be a promising thermoelectric material [6–8], a spin-orbit derived giant magnetoresistance [9] and a spontaneous anomalous Hall effect driven by topological effects [10] have been reported in this system as well. The Cr atoms host $S = 3/2$ spins arranged on a triangular lattice in each layer. The competing exchange interactions between the first- and third-nearest neighbour Cr moments lead to an incommensurate magnetic order at $T_N \approx 32$ K [11].

In this article, we report the concurrent emergence of Kondo behaviour in the temperature and field dependence of the in-plane electrical resistivity and incommensurate magnetic order of the Cr spins in AgCrSe₂. On the same temperature scale as this magnetic ordering, impurity Kondo behaviour emerges. Essential to understand this is the $\approx 1\%$ off-stoichiometry of the Cr ions,

detected by high-resolution wavelength X-ray diffraction spectroscopy, in our sample. The hybridization of the charge carriers at the Fermi level, dominated by the Se $4p$ states, with the Cr $3d^3$ states of these excess impurities would in principle lead to Kondo physics at low enough temperatures. However, above T_N , strong in-plane ferromagnetic fluctuations inhibit the hybridization between itinerant electrons and excess impurities. Only in the incommensurate magnetic order regime, at lower temperatures, an effective Kondo hybridization can exist. The key finding of our work—Kondo screening is enabled and associated with the antiferromagnetic order—opens an alternative route to tune the competition between the magnetic correlations and Kondo effect, which plays a central role in the heavy-fermion systems [12] and unconventional superconductors [13–15].

RESULTS

Electronic and magnetic structure of AgCrSe₂

High quality AgCrSe₂ single crystals were obtained via chemical transport reaction, and the growth process is described in detail in Baenitz et al. [11]. The crystal structure of the AgCrSe₂ single crystal is comprised of alternating layers of Ag and edge-sharing tilted distorted CeSe₆ octahedra [11, 16–18] that repeat along the crystallographic c axis (Fig. 1a-c). This crystal structure is very similar to the one that characterizes delafossite metals ($R\bar{3}m$) [19], however, there is no centrosymmetric inversion symmetry in this space group: $R3m$. The Cr atoms host $S = 3/2$ spins arranged on a triangular lattice in each layer [11]. Neutron measure-

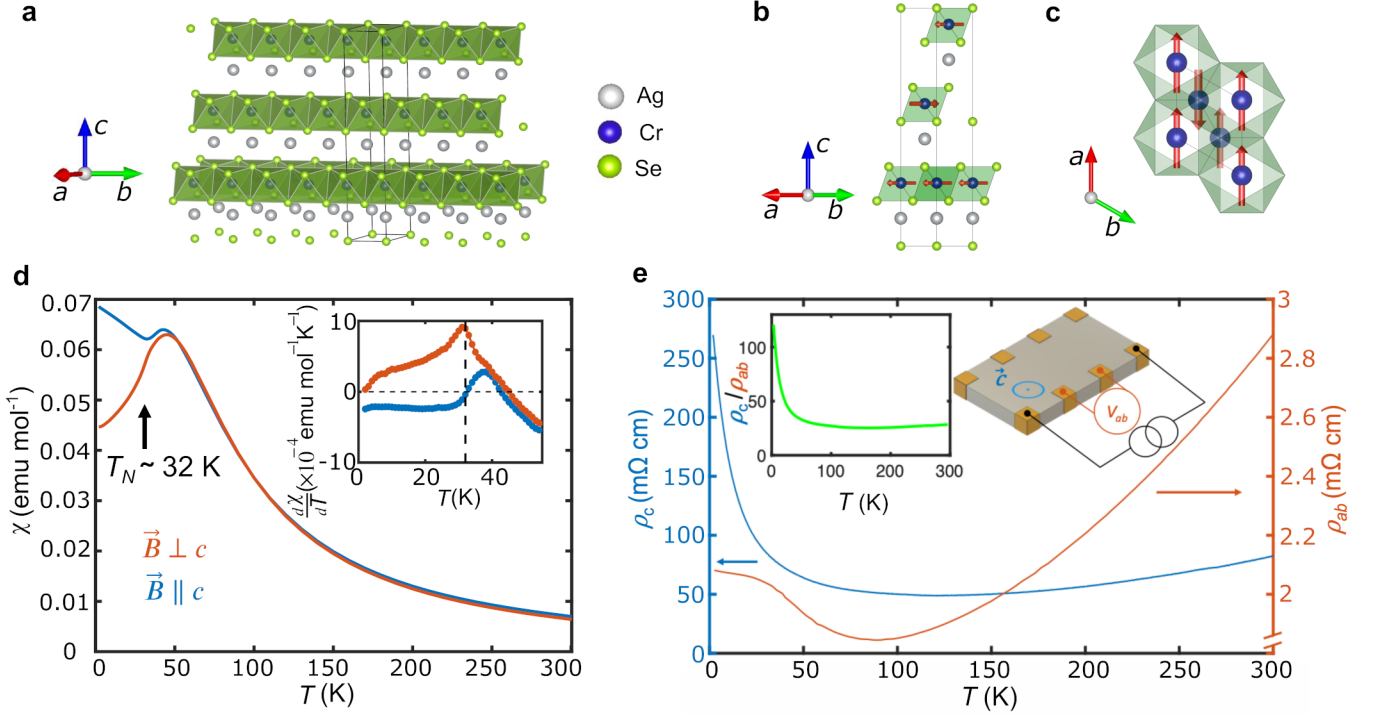


FIG. 1. **2D crystal structure and characteristic resistivity of AgCrSe₂.** **a** Crystal structure of AgCrSe₂, space group R3m. The translucent green polyhedra illustrate the tilted and distorted edge-sharing octahedra forming the triangular lattices. **b** Side view of the unit cell, including the Cr atoms spin that arrange antiferromagnetically along the *c* direction. **c** Bottom view of the unit cell showing the ferromagnetically alignment in the *ab* plane, in this simplification the long wavelength cycloidal periodicity discussed in Baenitz *et al.* [11] is ignored. **d** Magnetic susceptibility measured with a 1 T magnetic field in the *ab* plane, orange line, and along the *c* axis, blue line, and its derivative with respect to temperature in the inset, following the same color code. The black arrow is pointing to a kink in the magnetic susceptibility, revealing the Néel transition temperature, T_N . This is the same temperature represented by the vertical black line depicted in the inset. **e** Temperature dependence of the resistivity of the AgCrSe₂ single crystal in the *ab* plane, orange line, along the *c* axis, blue line, and their ratio in the inset, green line.

ments evidence an incommensurate magnetic order below $T_N = 32$ K with ordering vector $\mathbf{Q} = (0.037, 0.037, 3/2)$ in units of the reciprocal lattice constants. Below T_N , the Cr³⁺ moments order almost ferromagnetically in the triangular plane (positive single-ion anisotropy) in a cycloidal fashion with an antiferromagnetic stacking perpendicular to the plane [11]. This value for the Néel temperature [20] is consistent with the temperature dependence of the magnetic susceptibility, χ , depicted in Fig. 1d, and previously discussed in [10, 11]. High quality AgCrSe₂ single crystals were obtained via chemical transport reaction, and the growth process is described in detail in Baenitz *et al.* [11]. The crystal structure of the AgCrSe₂ single crystal is comprised of alternating layers of Ag and edge-sharing tilted distorted CeSe₆ octahedra [11, 16–18] that repeat along the crystallographic *c* axis (Fig. 1a-c). This crystal structure is very similar to the one that characterizes delafossite metals (R3m) [19], however, there is no centro-symmetric inversion symmetry in this space group: R3m. The Cr atoms

host $S = 3/2$ spins arranged on a triangular lattice in each layer [11]. Neutron measurements evidence an incommensurate magnetic order below $T_N = 32$ K with ordering vector $\mathbf{Q} = (0.037, 0.037, 3/2)$ in units of the reciprocal lattice constants. Below T_N , the Cr³⁺ moments order almost ferromagnetically in the triangular plane (positive single-ion anisotropy) in a cycloidal fashion with an antiferromagnetic stacking perpendicular to the plane [11], as depicted in Fig. 1b,c. This value for the Néel temperature [20] is consistent with the temperature dependence of the magnetic susceptibility, χ , depicted in Fig. 1d, and previously discussed in Baenitz *et al.* and Kim *et al.* [10, 11].

Anisotropic transport properties of AgCrSe₂ under the influence of magnetic field

In order to study the electrical transport properties of the single crystal, a standard four-probe method was used in measuring a millimeter sized sample [21, 22].

In Fig. 1e, we present the temperature dependence of the resistivity both in the ab plane and perpendicular to it (note the different scales). We observe a strong anisotropy in the resistivity (inset of Fig. 1e), along the c direction, at $T \approx 2$ K, the resistivity is around two orders of magnitude higher than the in-plane resistivity, as expected for such a quasi two-dimensional (2D) layered compound [23]. This anisotropy has been previously discussed [11, 24] and suggests that the origin of the current along c , at the temperature range considered, are thermally activated Se states that dominate the density of states near the Fermi surface [8, 11].

The resistivity along the c axis shows a typical semiconductor behaviour: metallic-like temperature dependence at higher temperatures with the resistivity decreasing with decreasing temperature up to the point, at around 80 K, where the thermally activated conductors freeze out, revealing the intrinsic insulating character of the material. On the other hand, the ab plane resistivity depicts an interesting and yet to be discussed feature: Similar to the c plane resistivity, the ab plane resistivity decreases with the decrease of temperature and at lower temperatures starts increasing. This would again be typical of a semiconductor, however here we observe that this low-temperature increase saturates, motivating us to perform a more detailed investigation of the in-plane resistivity at lower temperatures.

We now focus on the resistivity increase and saturation at temperatures below the resistivity minimum. The ab plane resistivity measurements as a function of temperature were repeated at different values of an applied magnetic field perpendicular to the triangular plane. From Fig. 2a,b, we see that by applying a magnetic field the upturn in resistivity with the decrease of temperature is gradually suppressed. Furthermore, for high enough fields, 14 T, the upturn is fully suppressed with AgCrSe_2 showing a metallic behaviour in the entire temperature range. The possibility of manipulating the phenomena with field indicates that the origin of the upturn might be magnetic in nature.

Single-ion Kondo effect in the ab plane resistivity of AgCrSe_2

A possible mechanism to explain the data observed is the single-ion Kondo effect [25]. As an experimentally motivated model, it was first used to describe the observation that the resistivity of some metals containing magnetic impurities deviates at low temperatures from a monotonous decrease but instead has a minimum at a certain temperature. Furthermore, at temperatures below the minimum a logarithmic increase is observed followed by saturation. This increase can be attributed to the appearance of additional magnetic exchange scattering between electrons at the Fermi level and localized

magnetic moments substantially below it. Computing the scattering probability for conduction electrons in the Kondo model, a $-\ln(T)$ increase in resistivity with temperature is obtained [25] below the minimum temperature. Furthermore, as temperature approaches $T \gtrsim 0$ K, there is a crossover from the $-\ln(T)$ scaling [26] towards saturation.

In order to discuss the viability of the single-ion Kondo model to describe the resistivity behaviour observed, the resistivity was measured at magnetic fields between -9 T and 9 T, observing that for fields higher than 7 T, there is no visible Kondo effect. For fields between -7 T and 7 T, there clearly is a $-\ln(T)$ dependence for temperatures below the temperature at which the resistivity is minimum.

The resistivity for very low temperatures deviates from the $-\ln(T)$ scaling: this crossover to saturation can be taken as an approximation of the Kondo temperature T_K [27–29]. With the rich variety of systems revealing Kondo-like transport, there have been a wide number of numerical and analytical techniques that aim to quantitatively determine the Kondo temperature based on resistivity measurements [27, 30–32]. Innocently looking, obtaining quantitative results from the Kondo model is a seemingly complex task and often requires bold simplifications. In this sense, the determination of the Kondo temperature scale from only the resistivity behaviour should be taken as an approximate estimate rather than an exact temperature.

From the electrical transport measurements, the Kondo temperature of AgCrSe_2 is $T_K \approx 34$ K at $\mu_0 H = 0$ T. Although the magnetic field suppresses the upturn, the variation of the Kondo temperature itself with different magnetic fields is very small, see Fig. 2c, and shows that the strength of the Kondo effect remains essentially robust with field until it is fully suppressed at a certain critical field. The resistivity measurements were performed in magnetic fields in both perpendicular directions to the ab plane to exclude inhomogeneity and misalignment effects.

The behaviour of the resistivity in applied magnetic fields shown in Fig. 2b is also qualitatively explained [33] in terms of the Kondo effect, which is suppressed when the external applied magnetic field polarizes the impurity's spin, i. e., when the Zeeman energy of the impurity spin is of the order of the characteristic energy scale for the Kondo effect [34]. In our case, with an impurity spin $S = 3/2$ and a characteristic temperature $T_K \approx 34$ K, the corresponding crossover field necessary to suppress the Kondo effect is $\mu_0 H \approx 8$ T, which is in good agreement with the observed results.

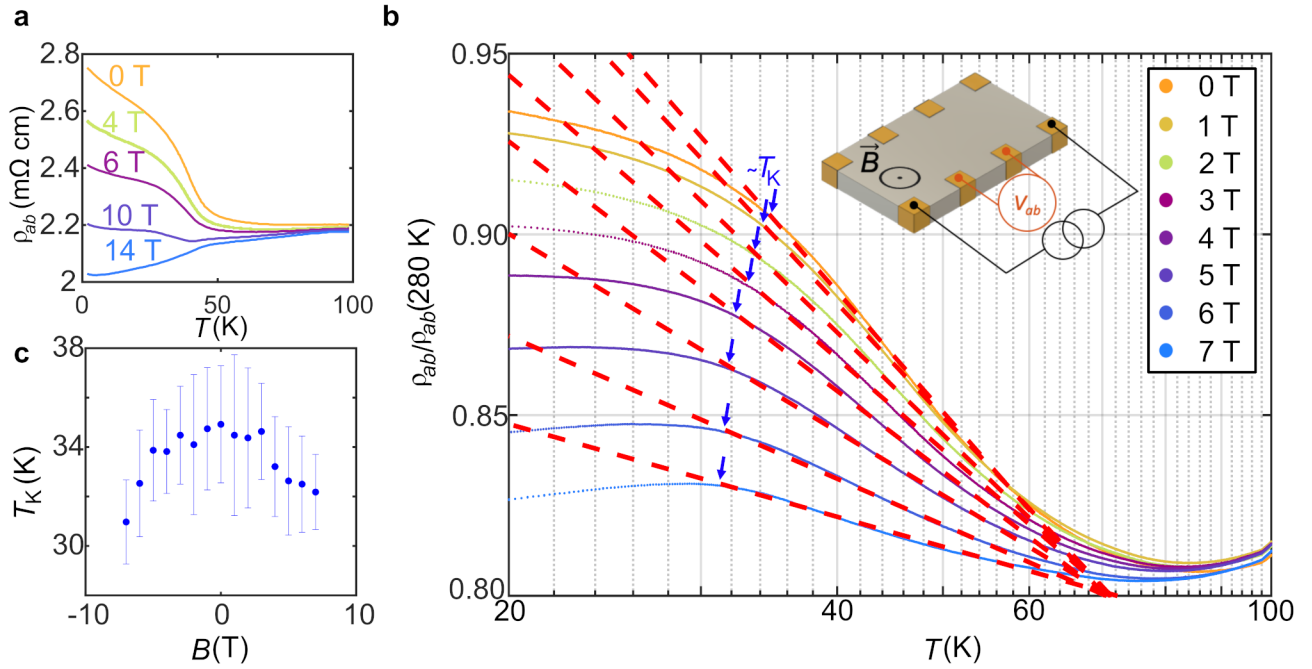


FIG. 2. **In-plane resistivity of AgCrSe₂ as a function of temperature under perpendicular magnetic fields.** **a** *ab* plane resistivity as a function of temperature with different applied out of plane magnetic fields $\mu_0 H = 0 \dots 14$ T. With a large enough field of $\mu_0 H \gtrsim 14$ T metallic behaviour can be observed in the entire temperature range $2 \text{ K} \leq T \leq 100 \text{ K}$. **b** Normalized *ab* plane resistivity as a function of temperature, showing the $-\ln(T)$ dependence at intermediate temperatures characteristic of the Kondo effect. The red dashed lines correspond to this logarithmic temperature dependence. The blue arrows point at the approximate value of T_K , the Kondo temperature value is estimated as the temperature at which the resistivity deviates from the logarithmic behaviour. **c** Variation of the Kondo temperature estimated from the resistivity measurements as a function of the out of plane magnetic field $\mu_0 H = -7 \text{ T} \dots 7 \text{ T}$, showing a small and symmetric variation around $H = 0$. The values shown are an average of repeated measurements and the error bars represent the standard error of the mean.

Magnetic field dependence of the Kondo effect: Schlottmann's scaling

The Kondo effect can also be observed in the magnetic field dependence of the resistivity of AgCrSe₂. According to Schlottmann's work on the Kondo model [35], the exchange scattering is dominated by a single energy scale related to $k_B T_K$ if the Kondo behaviour originates from scattering off localised magnetic impurities. This relation provides a much better definition for T_K and it is a property unique to the impurity Kondo model. By solving the Coqblin-Schrieffer Hamiltonian [36] using the Bethe Ansatz technique, for a given value of the impurity spin S the magnetoresistivity of a Kondo system was shown to have a universal scaling behaviour with field and temperature. The scaling field $B^*(T)$ depends on the Kondo temperature T_K according to $B^*(T) = B^*(0) + k_B T / (g\mu) = k_B (T_K + T) / (g\mu)$ where g is the Landé factor and μ is the expected moment of the localised magnetic impurity.

We make use of this universal relation as follows. First we measure the field dependence of the resistivity for different temperatures below the Kondo minimum (as depicted in Fig. 3a) and scale them to the theoretical

curve calculated by Schlottmann [35]. By fitting the scaled data with theoretical curves at different values of S , therefore μ , the relation allows a determination of the impurity spin S from the quality of the overlap between the scaled magnetoresistivity measured at each temperature and the theoretically expected value. The observed data scaling collapse is good, and agrees well with the scaling curve for $S = 3/2$, shown in Fig. 3b.

Second we obtain $B^*(0)$ from the scaling behaviour extrapolated to zero temperature. Knowing the value for S , that can be used to independently determine the Kondo temperature. The linear fit of the scaling field variation with temperature is shown in the inset of Fig. 3b. In summary, using Schlottmann's scaling, a value $S = 3/2$ is consistent with the experimental data and a Kondo temperature $T_K = (32 \pm 2) \text{ K}$ is obtained.

Emergence of Kondo behaviour and the relation to the incommensurate magnetic order of the Cr spins

In the section above, we have shown by measuring the temperature dependence of the electrical resistivity under a constant external magnetic field and the magne-

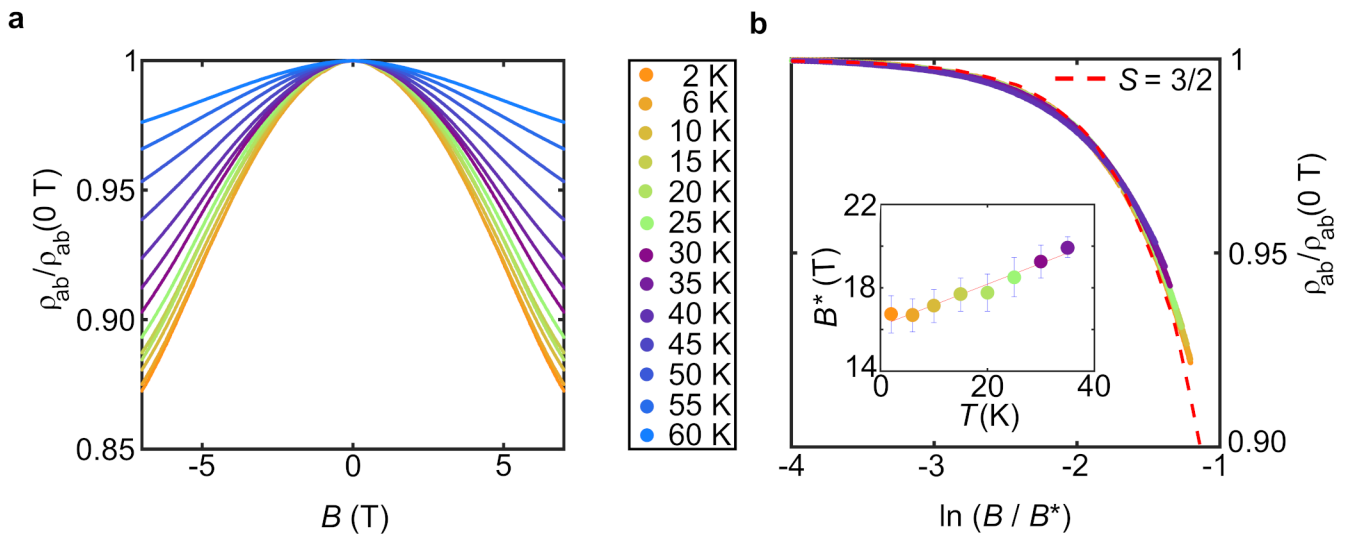


FIG. 3. **Schlottmann's scaling and magnetoresistivity.** **a** Normalized resistivity as a function of magnetic field at different temperatures T between 2 K and 60 K. The resistivity has been measured along the ab plane and normalised to the resistivity measured for each temperature with no applied magnetic field. **b** Normalized magnetoresistivity as a function of $\ln(B/B^*)$ for fields between -5 T and 5 T and temperatures up to 35 K. The fit parameter B^* is the scaling field, discussed in the 'Magnetic field dependence of the Kondo effect: Schlottmann's scaling' subsection of the Results. The theoretically expected curve [35] is marked by a red dashed line. Inset to **b** Scaling field $B^*(T)$ obtained from the fit of the normalized resistivities to the theoretical curve for temperatures from 2 K up to 35 K. The error bars represent the values of the scaling field within which the coefficient of determination between the theoretical curve and the scaled experimental data is higher or equal than 0.95.

toresistivity at different temperatures that the observed resistivity behaviour at low temperatures in the ab plane shows the hallmarks of a Kondo system, with a characteristic temperature $T_K \approx 32$ K. The Schlottmann scaling fit shown in Fig. 3b indicates that the magnetic impurities that drive the effect have a spin $S = 3/2$.

To investigate the origin of Kondo effect, wavelength X-ray dispersion measurements were performed in order to determine the crystal's elemental composition and concentration with high accuracy. The results shown in Table I indicate that the crystal has an off stoichiometry of $\text{Ag}_{0.942 \pm 0.004} \text{Cr}_{1.013 \pm 0.004} \text{Se}_2$. This composition was obtained taking into consideration the percentage weight at the perfect stoichiometry and normalized weights assuming a perfect concentration of Se. Furthermore the stoichiometry calculated is consistent with the carrier density obtained in Hall effect measurements [10].

The off-stoichiometry of Cr atoms is significant enough to be the origin of the Kondo effect, as only a very dilute concentration of the magnetic impurities is needed to observe a resistivity minimum [37]. Moreover, the Kondo effect has been previously reported elsewhere in antiferromagnetic materials with an excess of magnetic dopants [29].

From Table I we learn that the observed excess of Cr ions is accompanied by a lack of Ag ions. Therefore the most natural locations for the extra Cr impurities are silver vacancies.

From the ARPES data [8], we know that the states

TABLE I. **Wavelength-dispersive X-ray measurement of single crystal AgCrSe_2 .** The elemental information obtained from this spectroscopy measurement, weight and atomic percentage and their respective errors (Δ), reveals that the crystal does not have a perfect stoichiometry: having extra Cr ions and lacking Ag ions.

	Weight (%)	Δ Weight (%)	Atomic (%)	Δ Atomic (%)
Ag	33.043	0.117	24.815	0.063
Cr	17.132	0.044	25.616	0.054
Se	51.360	0.110	50.569	0.077

near the Fermi surface are dominated by the Se $4p$ states. It is to those conduction bands that the impurity Cr atoms couple, leading to Kondo physics, as represented in the schematic in Fig. 4.

DISCUSSION

The puzzling question that we now tackle is why we have $T_N = T_K$ and why the magnetic order actually induces the Kondo physics we observe in our transport measurements. As far as we are aware, this is the first system where the Néel temperature and the Kondo temperature coincide. The Néel temperature is a critical temperature that determines a magnetic phase transition. In contrast, the Kondo temperature does not represent a phase transition but rather represents an energy

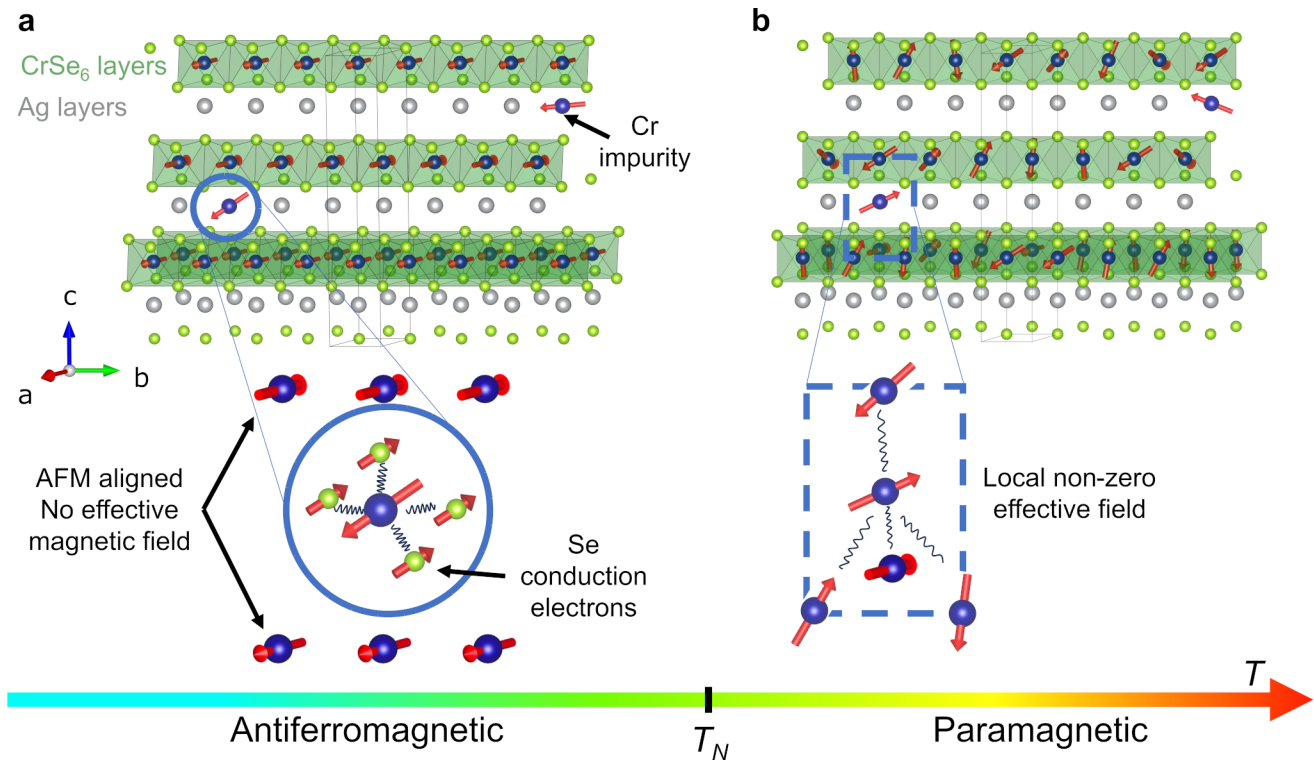


FIG. 4. **Schematic of the magnetic interactions that determine the concurrence of Kondo effect and the incommensurate magnetic arrangement of the Cr atoms.** Schematic illustration of the mechanisms behind the Kondo effect, highlighting the magnetic arrangements and interactions in play and how they differ in the **a** antiferromagnetic regime, at temperatures below the Néel temperature and **b** paramagnetic regime at higher temperatures. It is within this physical picture that the dependence of the Kondo regime on the antiferromagnetic transition becomes clear: as only at lower temperatures there is no effective magnetic field at the impurities sites and the impurity Kondo scattering can be observed. Simplification of the magnetic structure model, it does not reflect the cycloidal ordering discussed in Baenitz et al. [11] which is not important in our context.

scale for magnetic scattering of conduction electrons with magnetic impurities deep below the Fermi level, unrelated to magnetic order.

The magnetic structure of stoichiometric AgCrSe₂ is characterized by the Cr atoms that host a spin $S = 3/2$ in a $3d^3$ configuration [11, 38]. The Cr atoms in each layer form a triangular lattice and interact predominantly ferromagnetically within the ab plane. Out of the plane, adjacent layers of Cr atoms couple antiferromagnetically. Magnetic susceptibility measurements [11] yield an ordering temperature of $T_N = 32$ K.

In the paramagnetic phase above T_N , strong ferromagnetic fluctuations of the Cr spins in the CrSe₂ layers [11] induce nonzero effective magnetic fields in the Ag planes where also the excess Cr impurities are located. Due to this, time reversal symmetry is broken at the impurity sites and the Kondo coupling with the conduction electrons is strongly suppressed. At T_N , static magnetic order sets in: in the ab plane, the Cr spins order in a cycloidal fashion, however along the c direction, Cr spins are ordered antiferromagnetically. This static antiferro-

magnetic arrangement along c effectively cancels the induced magnetic fields in the Ag plus Cr impurities planes intercalated between the CrSe₂ layers, therefore allowing for the Kondo effect to emerge on the same energy scale as the antiferromagnetism.

The insights we gained here enable the study of systems from across the Doniach phase diagram [12] via impurity physics, even within the Kondo limit. It would be interesting to further explore the intricate interplay of magnetic interactions, such as the Ruderman-Kittel-Kasuya-Yosida interaction and various forms of magnetic scattering, across the phase diagram. Furthermore, it is important to contextualize our data within the Kondo framework, the concurrence of T_N and T_K is only possible in the Kondo single-ion model. In the traditional scenarios of competition between magnetic order and Kondo screening, such as the Kondo lattice model [12] and the Kondo necklace model [39], the appearance of magnetic order suppresses the Kondo effect.

To summarize, we have measured in detail the electronic transport properties of AgCrSe₂ at varying mag-

netic fields and temperatures. We observed a highly anisotropic resistivity, characteristic of a layered material. Careful analysis of the in-plane resistivity revealed an impurity Kondo behaviour with a characteristic temperature of $T_K \approx 34$ K in zero external magnetic field and a Kondo breakdown field consistent with both the estimated Kondo temperature and an impurity spin $S = 3/2$.

Magneto-resistance measurements confirmed the Kondo like transport with a characteristic temperature of $T_K \approx 32$ K, and the excellent agreement with the theoretically expected behaviour allows us to conclude that the magnetic impurities (i) are the origin of the Kondo scattering and (ii) have spin $S = 3/2$ in accordance with the value obtained from the Kondo breakdown field.

Finally we have discussed the relation between the antiferromagnetic order at T_N and the Kondo impurity scattering. To the best of our knowledge, our results uncovered a unique feature of AgCrSe_2 : the Néel temperature and the Kondo temperature coincide. We present a consistent physical picture of the mechanism behind that observation based on the location of the impurities and the cancellation of effective internal magnetic fields at these locations due to the onset of magnetic order, needed for the emergence of the impurity Kondo physics we observe in our magnetotransport measurements. Furthermore, our work would stimulate future studies to tune the interplay between Kondo screening and antiferromagnetic correlations on similar layered compounds.

METHODS

Device preparation

Single crystals of AgCrSe_2 were grown via chemical vapor transport techniques, following the methodologies outlined in Baenitz et al [11]. A device was fabricated with a single crystal of length ≈ 2 mm, width ≈ 1 mm and a thickness ≈ 50 μm , the contacts were deposited by sputtering gold in the crystal whilst it was covered by a shadow mask.

Transport measurements

Transport measurements were carried out in Helium-4 cryostats, equipped with a 9 T and a 14 T magnet, respectively. SR830 lock-in amplifiers were used to perform four-point resistance measurements. An alternating current was applied between the source and drain contacts, and the transverse and longitudinal voltages were measured simultaneously. We used the standard procedure of symmetrizing the longitudinal resistivity, $\rho_{ab}(H_{\rightarrow}) + \rho_{ab}(-H_{\leftarrow})/2 = \rho_{ab}$, where $H_{\rightarrow, \leftarrow}$ refers to the field sweep direction.

Magnetization measurements

Magnetization measurements were performed using a commercial vibrating sample magnetometer (VSM, Quantum Design).

X-ray spectroscopy

The stoichiometry of AgCrSe_2 was determined by EDX (energy dispersive x-ray spectroscopy) [40] analysis on a metallographically mounted and polished crystal. The analyses were performed on a scanning electron microscope (Jeol JSM 7800 F) with attached EDX (energy dispersive X-ray spectroscopy) system (Bruker Quantax 400). The stoichiometry results were confirmed and measured with higher precision making use of wavelength dispersive x-ray measurements.

DATA AVAILABILITY

All relevant data presented in the Manuscript are available from the corresponding author upon reasonable request.

CODE AVAILABILITY

All code relevant in analysing the data presented in the Manuscript are available from the corresponding author upon reasonable request.

REFERENCES

-
- * Correspondence: haijing.zhang@cpfs.mpg.de
- [1] F. Damay, S. Petit, M. Braendlein, S. Rols, J. Ollivier, C. Martin, and A. Maignan, Spin dynamics in the unconventional multiferroic AgCrS_2 , *Physical Review B* **87**, 10.1103/PhysRevB.87.134413 (2013).
 - [2] M. Matsuda, S. E. Dissanayake, H. K. Yoshida, M. Isobe, and M. B. Stone, Magnetic excitations affected by spin-lattice coupling in the $S = 3/2$ triangular lattice antiferromagnet Ag_2CrO_2 , *Phys. Rev. B* **102**, 214411 (2020).
 - [3] M. N. Baibich, J. M. Broto, A. Fert, F. N. Van Dau, F. Petroff, P. Etienne, G. Creuzet, A. Friederich, and J. Chazelas, Giant magnetoresistance of (001)Fe/(001)Cr magnetic superlattices, *Phys. Rev. Lett.* **61**, 2472 (1988).
 - [4] T. Ideue, S. Koshikawa, H. Namiki, T. Sasagawa, and Y. Iwasa, Giant nonreciprocal magnetotransport in bulk

- trigonal superconductor PbTaSe₂, *Phys. Rev. Res.* **2**, 042046 (2020).
- [5] A. Fert, N. Reyren, and V. Cros, Magnetic skyrmions: advances in physics and potential applications, *Nature Reviews Materials* **2**, 1 (2017).
- [6] D. Wu, S. Huang, D. Feng, B. Li, Y. Chen, J. Zhang, and J. He, Revisiting AgCrSe₂ as a promising thermoelectric material, *Phys. Chem. Chem. Phys.* **18**, 23872 (2016).
- [7] Y. Shiomi, T. Akiba, H. Takahashi, and S. Ishiwata, Giant piezoelectric response in superionic polar semiconductor, *Advanced Electronic Materials* **4**, 1800174 (2018).
- [8] Y. Hua, W. Bai, S. Wang, Y. Wu, S. Cui, Z. Sun, and C. Xiao, Tuning the electric transport behavior of AgCrSe₂ by intrinsic defects, *Science China Chemistry* **64**, 1970 (2021).
- [9] H. Takahashi, T. Akiba, A. H. Mayo, K. Akiba, A. Miyake, M. Tokunaga, H. Mori, R. Arita, and S. Ishiwata, Spin-orbit-derived giant magnetoresistance in a layered magnetic semiconductor AgCrSe₂, *Phys. Rev. Mater.* **6**, 054602 (2022).
- [10] S.-J. Kim, J. Zhu, M. M. Piva, M. Schmidt, D. Fartab, A. P. Mackenzie, M. Baenitz, M. Nicklas, H. Rosner, A. M. Cook, R. González-Hernández, L. Šmejkal, and H. Zhang, Observation of the anomalous Hall effect in a layered polar semiconductor, *Advanced Science*, 2307306 (2023).
- [11] M. Baenitz, M. M. Piva, S. Luther, J. Sichelschmidt, K. M. Ranjith, H. Dawczak-Dębicki, M. O. Ajeesh, S.-J. Kim, G. Siemann, C. Bigi, P. Manuel, D. Khalyavin, D. A. Sokolov, P. Mokhtari, H. Zhang, H. Yasuoka, P. D. C. King, G. Vinai, V. Polewczyk, P. Torelli, J. Wosnitzer, U. Burkhardt, B. Schmidt, H. Rosner, S. Wirth, H. Kühne, M. Nicklas, and M. Schmidt, Planar triangular $S = 3/2$ magnet AgCrSe₂: Magnetic frustration, short-range correlations, and field-tuned anisotropic cycloidal magnetic order, *Phys. Rev. B* **104**, 134410 (2021).
- [12] A. C. Hewson, *The Kondo Problem to Heavy Fermions* (Cambridge University Press, Cambridge, 1993).
- [13] N. Nagaosa and P. A. Lee, Kondo effect in high- T_c cuprates, *Phys. Rev. Lett.* **79**, 3755 (1997).
- [14] D. J. Scalapino, A common thread: The pairing interaction for unconventional superconductors, *Rev. Mod. Phys.* **84**, 1383 (2012).
- [15] S. Paschen and Q. Si, Quantum phases driven by strong correlations, *Nature Reviews Physics* **3**, 9 (2021).
- [16] B. Li, H. Wang, Y. Kawakita, Q. Zhang, M. Feygenson, H. L. Yu, D. Wu, K. Ohara, T. Kikuchi, K. Shibata, T. Yamada, X. K. Ning, Y. Chen, J. Q. He, D. Vaknin, R. Q. Wu, K. Nakajima, and M. G. Kanatzidis, Liquid-like thermal conduction in intercalated layered crystalline solids, *Nature Materials* **17**, 226 (2018).
- [17] C. Wang and Y. Chen, Highly selective phonon diffusive scattering in superionic layered AgCrSe₂, *npj Computational Materials* **6**, 26 (2020).
- [18] G.-R. Siemann, S.-J. Kim, E. A. Morales, P. A. E. Murgatroyd, A. Zivanovic, B. Edwards, I. Marković, F. Mazzola, L. Trzaska, O. J. Clark, C. Bigi, H. Zhang, B. Achinuq, T. Hesjedal, M. D. Watson, T. K. Kim, P. Bencok, G. van der Laan, C. M. Polley, M. Leandersson, H. Fedderwitz, K. Ali, T. Balasubramanian, M. Schmidt, M. Baenitz, H. Rosner, and P. D. C. King, Spin-orbit coupled spin-polarised hole gas at the CrSe₂-terminated surface of AgCrSe₂, *npj Quantum Materials* **8**, 61 (2023).
- [19] A. P. Mackenzie, The properties of ultrapure delafossite metals, *Reports on Progress in Physics* **80**, 032501 (2017).
- [20] M. E. Fisher, Relation between the specific heat and susceptibility of an antiferromagnet, *The Philosophical Magazine: A Journal of Theoretical Experimental and Applied Physics* **7**, 1731 (1962).
- [21] L. J. van der Pauw, A method of measuring specific resistivity and Hall effects of discs of arbitrary shape, in *Semiconductor Devices: Pioneering Papers* (1991) pp. 174–182.
- [22] H. Zhang, C. Berthod, H. Berger, T. Giamarchi, and A. F. Morpurgo, Band filling and cross quantum capacitance in ion-gated semiconducting transition metal dichalcogenide monolayers, *Nano letters* **19**, 8836 (2019).
- [23] T. Valla, P. D. Johnson, Z. Yusof, B. Wells, Q. Li, S. M. Loureiro, R. J. Cava, M. Mikami, Y. Mori, M. Yoshimura, and T. Sasaki, Coherence-incoherence and dimensional crossover in layered strongly correlated metals, *Nature* **417**, 627 (2002).
- [24] R. Yano and T. Sasagawa, Crystal growth and intrinsic properties of ACrX₂ (A = Cu, Ag; X = S, Se) without a secondary phase, *Crystal Growth & Design* **16**, 5618 (2016).
- [25] J. Kondo, Resistance minimum in dilute magnetic alloys, *Progress of Theoretical Physics* **32**, 37 (1964).
- [26] A. A. Abrikosov, Electron scattering on magnetic impurities in metals and anomalous resistivity effects, *Physique Fizika* **2**, 5 (1965).
- [27] H. Suhl, Dispersion theory of the kondo effect, *Phys. Rev.* **138**, A515 (1965).
- [28] L. J. Zhu, S. H. Nie, P. Xiong, P. Schlottmann, and J. H. Zhao, Orbital two-channel kondo effect in epitaxial ferromagnetic L10-MnAl films, *Nature Communications* **7**, 10817 (2016).
- [29] D. Khadka, T. R. Thapaliya, S. H. Parra, X. Han, J. Wen, R. F. Need, P. Khanal, W. Wang, J. Zang, J. M. Kikkawa, L. Wu, and S. X. Huang, Kondo physics in antiferromagnetic weyl semimetal Mn_{3+x}Sn_{1-x} films, *Science Advances* **6**, eabc1977 (2020).
- [30] A. Tsvelick and P. Wiegmann, Exact results in the theory of magnetic alloys, *Advances in Physics* **32**, 453 (1983).
- [31] P. Coleman, New approach to the mixed-valence problem, *Phys. Rev. B* **29**, 3035 (1984).
- [32] N. E. Bickers, D. L. Cox, and J. W. Wilkins, Self-consistent large-N expansion for normal-state properties of dilute magnetic alloys, *Phys. Rev. B* **36**, 2036 (1987).
- [33] A. F. Otte, M. Ternes, K. von Bergmann, S. Loth, H. Brune, C. P. Lutz, C. F. Hirjibehedin, and A. J. Heinrich, The role of magnetic anisotropy in the Kondo effect, *Nature Physics* **4**, 847 (2008).
- [34] R. Žitko, R. Peters, and T. Pruschke, Splitting of the kondo resonance in anisotropic magnetic impurities on surfaces, *New Journal of Physics* **11**, 053003 (2009).
- [35] P. Schlottmann, Bethe-Ansatz solution of the ground-state of the SU(2j+1) Kondo (Coqblin-Schrieffer) model: Magnetization, magnetoresistance and universality, *Zeitschrift für Physik B Condensed Matter* **51**, 223 (1983).
- [36] B. Coqblin and J. R. Schrieffer, Exchange interaction in alloys with cerium impurities, *Phys. Rev.* **185**, 847 (1969).
- [37] J. Kondo, Sticking to my bush, *Journal of the Physical Society of Japan* **74**, 1 (2005).

- [38] F. M. R. Engelsman, G. A. Wiegers, F. Jellinek, and B. Van Laar, Crystal structures and magnetic structures of some metal(i) chromium(iii) sulfides and selenides, *Journal of Solid State Chemistry* **6**, 574 (1973).
- [39] A. Langari and P. Thalmeier, Antiferromagnetic and spin-gap phases of the anisotropic kondo necklace model, *Phys. Rev. B* **74**, 024431 (2006).
- [40] R. Fitzgerald, K. Keil, and K. F. J. Heinrich, Solid-state energy-dispersion spectrometer for electron-microprobe x-ray analysis, *Science* **159**, 528 (1968).

ACKNOWLEDGEMENTS

We thank A. P. Mackenzie, M. M. Piva, P. Thalmeier and U. Burkhardt for useful discussions, and S. Seifert for experimental support. J. Guimarães, D. Fartab and M. Moravec acknowledge support from the International Max Planck Research School for Chemistry and Physics of Quantum Materials (IMPRS-CPQM). We are grateful to the Max Planck Society for financial support.

AUTHOR CONTRIBUTIONS

J.G. and H.Z. conceived the research project. J.G., D.F. and H.Z. collaborated in the device fabrication. M.S. grew the single crystals. M.B. performed the magnetic susceptibility measurements. J.G. and H.Z. performed the electrical transport measurements, which were analysed by J.G.. J.G., M.M., B.S. and H.Z. were involved in many discussions to come up with the physical model that supported the observed data. H.Z. led the project and the paper was written by J.G., H.Z. and B.S., with input and comments by M.M. and M.B..

COMPETING INTERESTS

The authors declare no competing interests.